BRAIN CONNECTIVITY
Volume 9, Number 4, 2019

DOI: 10.1089/brain.2018.0640

Lower Limb Task-Based Functional Connectivity Is Altered in Stroke

Kaleb Vinehout,[1] Brian D. Schmit,[1] and Sheila Schindler-Ivens[2]

Abstract

The goal of this work was to examine task-dependent functional connectivity of the brain in people with stroke. The work was motivated by prior observations indicating that, during pedaling, cortical activation volume is lower in people with stroke than controls. During paretic foot tapping, activation volume tends to be higher in people with stroke than controls. This study asked whether these differences could be explained by altered network function of the brain. Functional magnetic resonance imaging was used to examine local and global network function of the brain during tapping and pedaling in 15 stroke and 8 control participants. Independent component analysis was used to identify six task regions of interest (ROIs) in the primary sensorimotor cortex (M1S1), anterior lobe of cerebellum (AlCb), and secondary sensory cortex (S2) on the lesioned and non-lesioned sides of the brain (left, right for controls). Global connectivity was calculated as the correlation between mean time series for each ROI. Local connectivity was calculated as the mean correlation between voxels within each ROI. Local efficiency, weighted sum, and clustering coefficient were also calculated. Results suggested that local and global networks of the brain were altered in stroke, but not in the same direction. Detection of both global and local network changes was task-dependent. We found that global network function of the brain was reduced in stroke participants as compared with controls. This effect was detected during pedaling and nonparetic tapping, but not during paretic tapping. Local network function of the brain was elevated in stroke participants during paretic tapping and reduced during pedaling. No between-group differences in local connectivity were seen during nonparetic tapping. Connections involving S2, M1S1, and AlCb were significantly affected. Reduced global connectivity of the brain might contribute to reduced brain activation volume during pedaling poststroke.

Keywords: fMRI; functional connectivity; locomotion; motor control; stroke; task-based

Introduction

Recently, our group used functional magnetic resonance imaging (fMRI) to examine brain activation during pedaling and foot tapping in people with stroke and age-matched controls (Promjunyakul et al., 2015). The comparison between pedaling and tapping was made to determine whether models of cortical control of unilateral, single-joint movement after stroke extend to bilateral, multijoint movements of the lower limbs. Although many recovery models include vicariation of function, our prior results indicate that vicariation does not extend to pedaling. Specifically, during paretic foot tapping, cortical activation volume tended to be higher in people with stroke than controls. This observation is consistent with prior work showing that the intensity or volume of brain activation is elevated during unilateral, single-joint movements of limbs (Calautti and Baron, 2003; Carey et al., 2004; Cramer et al., 1997; Enzinger et al., 2008; Fridman et al., 2004; Johansen-Berg et al., 2002; Kim et al., 2006). It supports the idea that motor recovery after stroke occurs through vicariation of function (Carey et al., 2004; Johansen-Berg et al., 2002; Kim et al., 2006) and other mechanisms whereby intact brain regions compensate for those damaged by stroke (Calautti and Baron, 2003; Cramer et al., 1997).

In contrast to the paretic tapping condition, brain activation volume during pedaling was significantly lower in people with stroke than controls (Promjunyakul et al., 2015). Reduced activation volume was seen in all brain regions activated by pedaling (i.e., M1, S1, supplemental motor area, and cerebellar lobules IV, V, and VIII). These observations cannot be attributed to between-group differences in movement rate, head motion, lesion size, or other methodological factors. From this prior study, we concluded that different neural adaptations might be associated with recovery of rhythmic and discrete movement and that detection of these adaptations might be task-dependent.

[1]Department of Biomedical Engineering, Marquette University and the Medical College of Wisconsin, Milwaukee, Wisconsin.
[2]Department of Physical Therapy, Marquette University, Milwaukee, Wisconsin.

The work presented here sought to determine whether altered network function of the stroke-affected brain could explain differences in activation volume during pedaling and tapping. We considered that unilateral, single-joint movements that involve one antagonist pair (e.g., tapping) might be accomplished with local networks that connect nearby processing units within discrete anatomical boundaries. Coordinated movement of both limbs across multiple joints (e.g., pedaling) might require global networks that connect anatomically distinct regions separated by long distances. Reduced brain activation volume during pedaling could be the result of loss of global network function after stroke, whereas increased brain activation during tapping might reflect an increase in local network function.

Though limited in number, studies of global network function of the stroke-affected brain provide preliminary support for a decrease in global connectivity after stroke (Westlake and Nagarajan, 2011). For example, Urbin et al. (2014) examined functional connectivity between regions of the sensorimotor network in chronic stroke survivors in the resting state. They found that the strength of homo- and heterotopic connections between hemispheres was lower in stroke participants than controls. Further, measures of functional connectivity are task-dependent. Task-dependent effective connectivity among regions of the motor cortex has been documented at rest and during whole-hand fist closing with the right, left, and both hands (Grefkes et al., 2008a,b). In able-bodied individuals, the strength and sign of neural coupling between motor areas is modulated by the task (i.e., rest, unilateral, bilateral). Moreover, the ability to detect differences in global network function between stroke and control groups is task-dependent.

In contrast to decreased global network function, local network function of the stroke-affected brain may be elevated. Yang et al. (2016) showed that local connectivity within language areas of the brain is higher in people with stroke as compared with healthy, age-matched individuals. This work was done in the resting state, and to our knowledge local network function associated with language areas of the stroke-affected brain has not been studied during a task. Hence, the extent to which local network function depends on task is unclear. Some work suggests no task-dependency in local network function. For example, a large meta-analysis of data from thousands of functional connectivity studies found that resting-state and task-based approaches fully identify local networks of the brain, including the sensorimotor network (Smith et al., 2009). Although this work identified local networks, it did not examine the strength of the functional connections within them. Moreover, it was done in unimpaired participants and results may not be the same in people with stroke.

In this study, global and local network connectivity during pedaling and foot tapping were measured to obtain additional insight into the brain activation patterns associated with these tasks. Global and local network function can be measured in a variety of different ways. Global network function has been measured by correlations of seed-based connectivity (Biswal et al., 1995), independent component analysis (ICA)-defined components time series (Smith et al., 2009), or of mean time series within a given region of interest (ROI; Roy et al., 2009). Local network function has been measured by an area's contribution to an ICA-defined component (Smith et al., 2009), or by the amplitude of low-frequency fluctuations of a given ROI (Yu-Feng et al., 2007). Here, the correlation of the mean time series of an ROI to other ROIs as a measure of global network function and the mean correlation of the voxel time series within an ROI as a measure of local networks were chosen. This measure of global network function was chosen to allow for all changes in connections to a distinct region to contribute to the functional connectivity measure. The measurement of local network function was chosen to allow for a computational simple measurement of spatially distinct networks.

In this study, global and local network function during pedaling and foot tapping in people with and without stroke was examined. Global connectivity was measured with Pearson correlation coefficients between ROIs of the brain, and local connectivity was measured based on voxel correlations within each ROI. Consistent with the framework described earlier, it was hypothesized that global network function would be reduced, and that local network function would be elevated in people with stroke as compared with controls. It was also predicted that the ability to detect these effects would be task-dependent. Pedaling was expected to reveal between-group differences in global network function (correlation between ROIs); tapping would reveal differences in local networks (correlation of voxels within each ROI). Support for these hypotheses would provide evidence that task-related differences in brain activation volume poststroke are associated with differential changes in global and local network function of the brain.

Methods

Participants

Fifteen individuals with stroke [nine females; mean (standard deviation or SD) age 55.6 (11.9) years] and eight controls [five females; age 53.4 (13.2) years] participated. All provided written informed consent according to the Declaration of Helsinki and institutional guidelines at Marquette University and the Medical College of Wisconsin. All were free from contraindications to magnetic resonance imaging (MRI), orthopedic injuries that could interfere with pedaling, and neurological conditions other than stroke. To be included, people with stroke had to have sustained their infarct at least 6 months before testing. The mean (SD) time since stroke was 12.2 (12.2) years. Cortical and subcortical strokes on either side of the brain were allowed. Eight stroke participants had subcortical lesions involving the internal capsule, corona radiata, basal ganglia, or thalamus. Seven stroke participants had lesions affecting a portion of the cerebral cortex. There were seven individuals with left- and seven with right-sided stroke. One stroke survivor had subcortical lesions on the right and left side. When this participant was enrolled, he reported a history of only one stroke and presented with right-sided lower limb impairment. The second lesion on the research scan was detected. Lesion locations are depicted in Figure 1. Clinical and demographic information is provided in Table 1.

Procedures and equipment

For brain imaging, participants were positioned supine on an MRI scanner bed. The head was placed in a radio

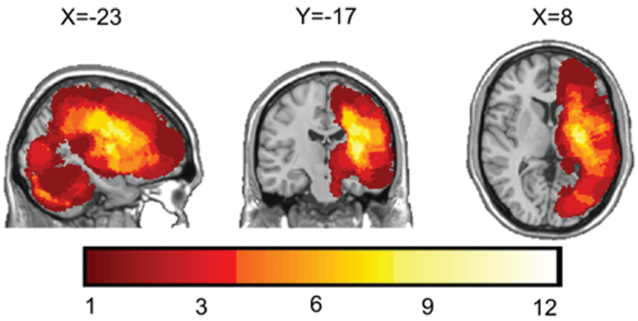

FIG. 1. Lesion location. Visual representation of lesion location among stroke participants. Colors represent the frequency with which a lesion affected a given voxel. Red represents voxels least frequently affected ($n = 1$ participant), and white represents voxels most frequently affected ($n = 12$ participants at $X = 118$, $Y = 113$, $Z = 82$). Note that at most only 12 of the 15 stroke participants had lesions in the same location. Lesions are shown in Montreal Neurological Institute space by using radiological convention. Right-sided lesions were flipped to the left. Color images are available online.

frequency coil and secured with a beaded vacuum pillow, chin strap, and other padding to minimize motion. The trunk was secured with a Velcro strap. MRI compatible ear buds delivered audio cues indicating when to move and rest. Pedaling and tapping were performed on different days; the order was counterbalanced.

During pedaling, the feet were fastened to a custom-designed device that was positioned at the end of the scanner bed. The device has been described and previously validated (Mehta et al., 2009). In brief, it was a direct-drive, flywheel-equipped apparatus instrumented with a rotary optical encoder coupled to the crank shaft. Participants performed six runs of pedaling at a comfortable rate. Each run comprised 30 sec of pedaling, followed by 30 sec of rest, repeated four times. Runs were preceded by 18 sec of rest. The total task time for pedaling was 25.8 min; 774 repetition times (TRs) were collected (Promjunyakul et al., 2015).

During tapping, the legs were positioned over a bolster such that the hip and knees were flexed and the feet were ~15 cm above the surface of the scanner bed. A circular button (6.35 cm diameter) connected to a switch (Jelly Bean Twist Top Switch; AbleNet, Inc., Roseville, MN) was placed under the foot. Participants were asked to dorsi- and plantarflex the ankle at a comfortable rate to tap the button. Knee flexion/extension was allowed if ankle movement was not possible. Tapping was performed with one limb at a time, once for left (paretic) and once for right (nonparetic). Tapping used an event-related design that consisted of three runs. A single run included 20 tapping events and 74 resting events with 2 sec per event, presented in random order. The total task time for tapping was 9.40 min per limb; 282 TRs were collected in this time (Promjunyakul et al., 2015).

A 3.0T MRI scanner and a single-channel transmit/receive split head coil were used (General Electric Healthcare, Milwaukee, WI). Functional images (T2*-weighted) were acquired by using echo planar imaging (TR: 2000 ms, echo time [TE]: 25 ms, flip angle: 77°, 36 contiguous slices in the sagittal plane, 64×64 matrix, 4 mm slice thickness, and field of view [FOV]: 240 mm). The resolution of the images was $3.75\,\text{mm} \times 3.75\,\text{mm} \times 4\,\text{mm}$. Anatomical images (T1-weighted) were obtained with a spoiled gradient recalled acquisition in the steady-state pulse sequence obtained approximately half way through scan sessions (TR: 9.6 ms, TE: 39 ms, flip angle: 12°, 256×244 matrix, resolution: $1\,\text{mm}^3$, FOV: 240 mm, 148 slices in the sagittal plane, and number of excitations: 1; Promjunyakul et al., 2015). People with stroke underwent an 8 m comfortable walk test. The lower extremity portion of the Fugl-Meyer Assessment was administered (Fugl-Meyer et al., 1975). The total score (FMLEtotal) was subdivided into motor (FMLEmotor) and sensory (FMLEsens) components.

Table 1. Clinical and Demographic Information on Stroke Participants

Subject ID	*Age (years)*	*Sex*	*Side of stroke*	*Affected brain area*	*Time since stroke (years)*	*Mechanism of stroke*	*FMLE total/ motor/sensory max = 56/44/12*	*Walking velocity (m/s)*
S01	60	F	L	Cort	20.4	I, E	39/37/2	1.10
S02	57	M	R	Cort	11.8	I	29/25/4	0.66
S03	62	F	R	Subcort	8.4	I	54/42/12	1.11
S05	56	M	R	Subcort	51.0	H, AVM	43/31/12	1.04
S06	64	F	L	Subcort	6.5	H	54/42/12	0.82
S07	20	F	R	Subcort	19.0	U	47/35/12	1.13
S08	73	F	L	Subcort	1.1	I, E	52/40/12	1.04
S10	58	F	R	Cort	6.1	I, CVOD	42/30/12	0.48
S11	53	F	L	Subcort	17.4	I	53/41/12	1.05
S12	62	M	L	Subcort	13.9	I	42/30/12	1.05
S13	46	M	L, R	Subcort	4.4	I	37/25/12	0.82
S14	52	F	R	Cort	3.0	H, ICAD	45/33/12	0.59
S15	51	M	L	Cort	8.1	H, ICAD	37/25/12	0.88
S17	65	F	R	Cort	6.2	I	26/24/2	0.20
S19	55	M	L	Cort	6.4	I, CVOD	53/41/12	1.22
Mean (SD)	55.6 (11.9)				12.2 (12.2)		44/33/10 (9/7/4)	0.88 (0.29)

AVM, arteriovenous malformation; Cort, stroke affecting cerebral cortex; CVOD, cerebrovascular occlusive disease; E, embolism; F, female; FMLE, Fugl-Meyer Lower Extremity; H, hemorrhage; I, ischemia; ICAD, internal carotid artery dissection; L, left; M, male; R, right; Subcort, stroke affecting subcortical white matter; U, unknown.

Preprocessing

T1-weighted images were skull stripped and registered to Montreal Neurological Institute space by using Brain Extraction Tool and Advanced Normalization Tools (ANTs), respectively (Avants et al., 2011; Smith et al., 2004). The same registration was applied to the fMRI data, after which these data were transposed so that all lesions were represented on the left side. fMRI time series data were temporally and spatially filtered (0.1 Hz high pass, 5 mm Gauss) in the fMRI Expert Analysis Tool. Motion-based noise was removed with ICA-based Automatic Removal of Motion Artifacts (ICA-AROMA) (Pruim et al., 2015).

Identification of task ROIs

These steps were used to provide ROIs that were representative of functional networks and encompassed the whole brain. In addition, task ROIs included areas related to task but not necessarily correlated with the hemodynamic response function (HRF). An overview of the analysis procedures is provided in Figure 2. After concatenating the fMRI time series across participants, groups, and conditions, ICA was performed by using the multivariate exploratory linear-optimized decomposition into independent components function in fMRI Brain Software Library. The number of independent components was estimated by using a Bayesian approach described by Minka (2001). It was decided not to constrain the number of components outside of this estimation to allow for more temporal separation between components. This process identified 79 components that were divided into sub-components by splitting each into a left and right half along the midline of the brain and then by applying an algorithm to identify spatially distinct subcomponents. The algorithm was applied to the thresholded *p*-values associated with the relationship between the individual voxel time series and the mixing matrix. This algorithm was applied

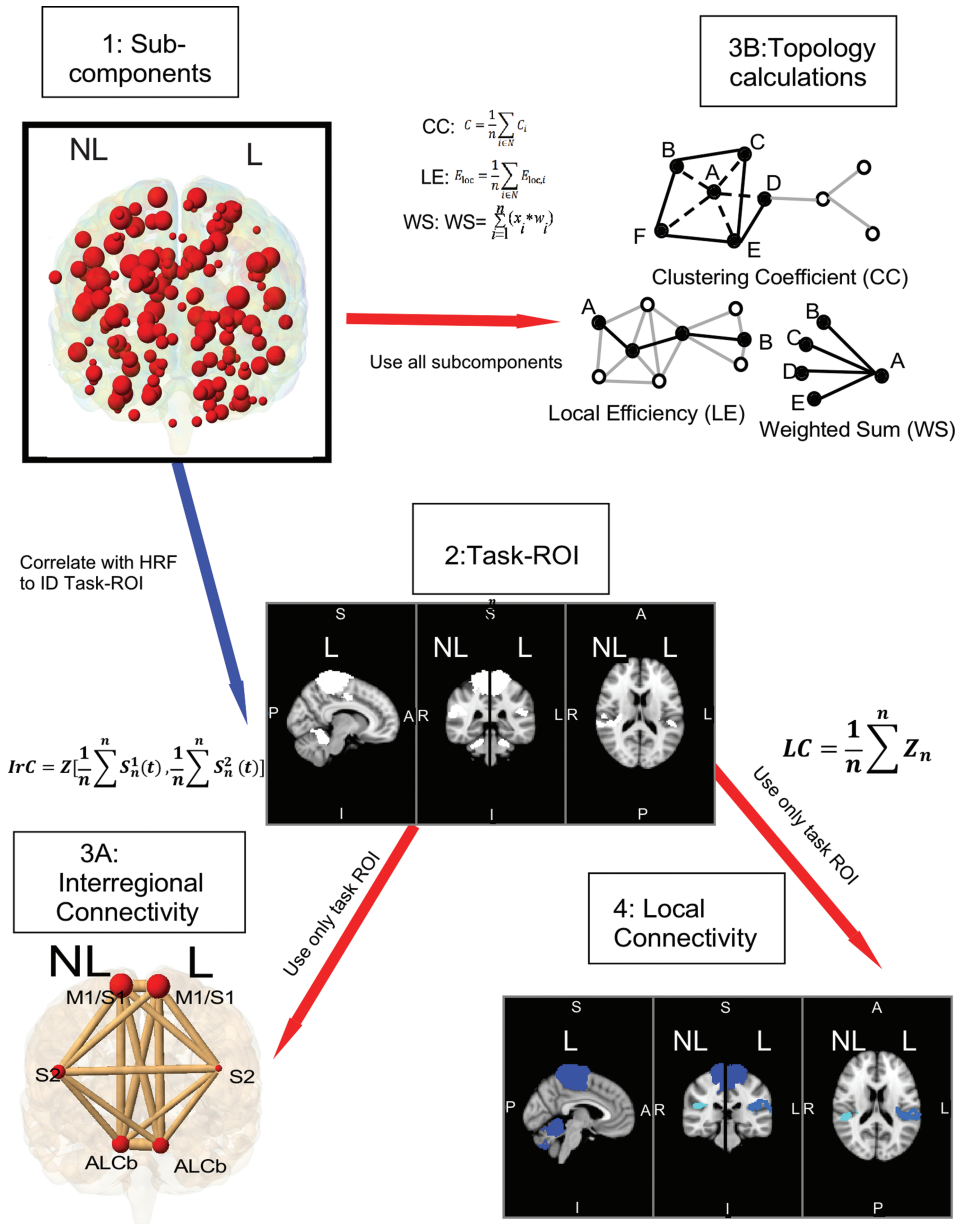

FIG. 2. Methods. Diagram of global and LC calculations. The 163 subcomponents defined by the spatiotemporal similarity of the voxels **(1)** are used in topology calculations **(3B)**. All 163 subcomponents time series data were correlated with the pedaling HRF to identify task ROIs **(2)**. Task ROIs were used to define interregional connectivity **(3A)** and LC **(4)**. In this figure, the red arrows indicate a step that used the fMRI data with the task regressed out, whereas the blue arrows indicate a step without the task regressed out of the fMRI data. In the equation for LC, *Z* represents the Fisher-*Z*-transformed correlation coefficient; *n* is the number of voxels in a region. For the inter-regional connectivity equation, $S_n^1(t)$ is the time series of the nth voxel in ROI 1; *Z* is the Fisher-*Z*-transformed correlation coefficient. ALCb, anterior lobe of cerebellum; CC, clustering coefficient; fMRI, functional magnetic resonance imaging; L, lesioned; LC, local connectivity; LE, local efficiency; M1S1, primary sensorimotor cortex; NL, non-lesioned; ROIs, regions of interest; S2, secondary sensory cortex; WS, weighted sum. Color images are available online.

to each of right or left 79 components individually; therefore, this algorithm was applied to 158 unique images. This allowed us to identify spatially distinct subcomponents within the left or right hemisphere of each component. Of the original 79 components, 32 were only in one hemisphere and 23 were split along the midline of the brain. The minimum subcomponent size was heuristically set to 1.1 cm with a p-value threshold of 0.05. This approach was selected to encompass all observable subcomponents, which was typically 1 or 2 per component. Finally, the white matter and non-brain components were regressed out. These processes left 163 subcomponents (Fig. 2–1). Pearson correlation coefficients were used to examine the association between each subcomponent and the HRF associated with pedaling. Subcomponents that were correlated with the HRF ($r > 0.50$) were considered task ROIs as were non-correlated subcomponents that were located within the same component as those that were task correlated (Fig. 2–2).

The HRF was regressed out of the original signal for subsequent analyses. The task-related changes in the fMRI time series were removed with general linear modeling by using 3dDeconvolve in Analysis of Functional NeuroImages (Cox, 1996). This process involved regressing the block design HRF from the pedaling data and the event-related design HRF from the tapping data. The remaining fMRI time series was used for connectivity analyses.

Measures of global connectivity

For each participant and task, a mean fMRI time series was computed for each of the six task ROIs. Pearson correlation coefficients were computed on all pairwise combinations of these data; Fischer-Z transformations were applied to the correlations. These values provided a measure of global connectivity that represented the strength of functional connections between task ROIs (Fig 2.3A). The five unique task ROI connections to each task ROI as inter-regional connectivity were defined. Global connectivity was also assessed by computing topology measures associated with each task ROI and all 163 subcomponents identified from the ICA. As with inter-regional connectivity, a mean time series was computed for each subcomponent. Pearson correlation coefficients were computed for all pairwise combinations of task ROIs and subcomponents. Fischer-Z transforms were applied. Per the methods of Rubinov and Olaf Sporns (2010), these values were used to compute the weighted sum (WS), local efficiency (LE), and clustering coefficient (CC) associated with each task ROI (Fig. 2–3B). These measures provided insight into the strength of the functional connections among task ROIs and all brain regions.

Measures of local connectivity

For each participant and task, Pearson correlation coefficients were computed for all pairwise combinations of voxel time series within each task ROI. Fisher-Z transformations were applied. For an ROI with n voxels, this gave a correlation matrix of size n by n. Local connectivity was defined as the mean of all Fischer-Z-transformed correlation coefficients of the correlation matrix for each task ROI, yielding one value for each ROI for each subject (Fig. 2–4).

Statistics

Values for inter-regional connectivity were organized into sets anchored to one task ROI. For example, a set of inter-regional connectivity data anchored to the primary sensorimotor cortex (M1S1) would include all the correlations between M1SI and all other task ROIs. Sets anchored to each task ROI were created for each condition. Two-way analysis of variance (ANOVA) was used to identify group and group by region effects for each set. Two-way ANOVA was also used to examine group and group by region effects on local connectivity. With respect to topology measures, two-way ANOVA was used to examine group, condition, and group by condition effects on the WS, LE, and CC. In the presence of significant group effects, partial eta-squared was used to compute effect size (ES). Associations between connectivity and clinical measures were assessed with Pearson correlation coefficients. Variables with significant between-group effects were used. In the case of inter-regional connectivity, only connections with the largest between-group effect were used. To determine the effect that the one stroke participant with bilateral lesions (S13) had on statistical tests, all tests were performed with and without this subject. All analyses were completed in Statistical Package for the Social Sciences (IBM Corp. Released 2016. IBM SPSS Statistics for Mac, Version 24.0.; IBM Corp., Armonk, NY) with $\alpha < 0.05$.

Results

Task ROIs

Six task ROIs were identified by the algorithm applied to the ICA of all the T2*-weighted data. Task ROIs were in the M1S1, anterior lobe of cerebellum (AlCb), and secondary sensory cortex (S2) on the lesioned (L) and non-lesioned (NL) sides of the brain (left, right for controls). See Supplementary Figure S1 for visual depiction of areas. Task ROIs in M1S1 and AlCb were correlated with the HRF. Task ROIs in S2 were not correlated with the HRF but were part of the component containing M1S1 and AlCb.

Global connectivity

During pedaling, inter-regional connectivity was lower in the stroke than the control group, as evidenced by a significant main effect of group for all six task ROIs ($p \leq 0.013$; Fig 3). In the set anchored to the NL S2, there was also a significant group by region interaction ($p = 0.027$). The interaction was due to a larger between-group effect for the connection between NL S2 and L S2, as compared with the other connections in this set (Fig. 3d). When this connection was removed from the set, there was no effect of group ($p = 0.338$). The set with the largest ES was the one anchored to L S2 (ES = 0.349, $p < 0.001$). For all other sets, the ES was ≤0.148 (Fig. 3b–f). Due to its large ES and potential influence on the sets anchored to other task ROIs, the L S2 dataset was removed, and statistical analyses were repeated. Without L S2, there was still a significant main effect of group for L M1S1, NL AlCb, and NL M1S1 ($p \leq 0.017$), but ES dropped to ≤0.088. No significant interactions were detected ($p \geq 0.653$).

As shown in Figure 4, inter-regional connectivity during non-paretic (NP) tapping was lower in the stroke group than

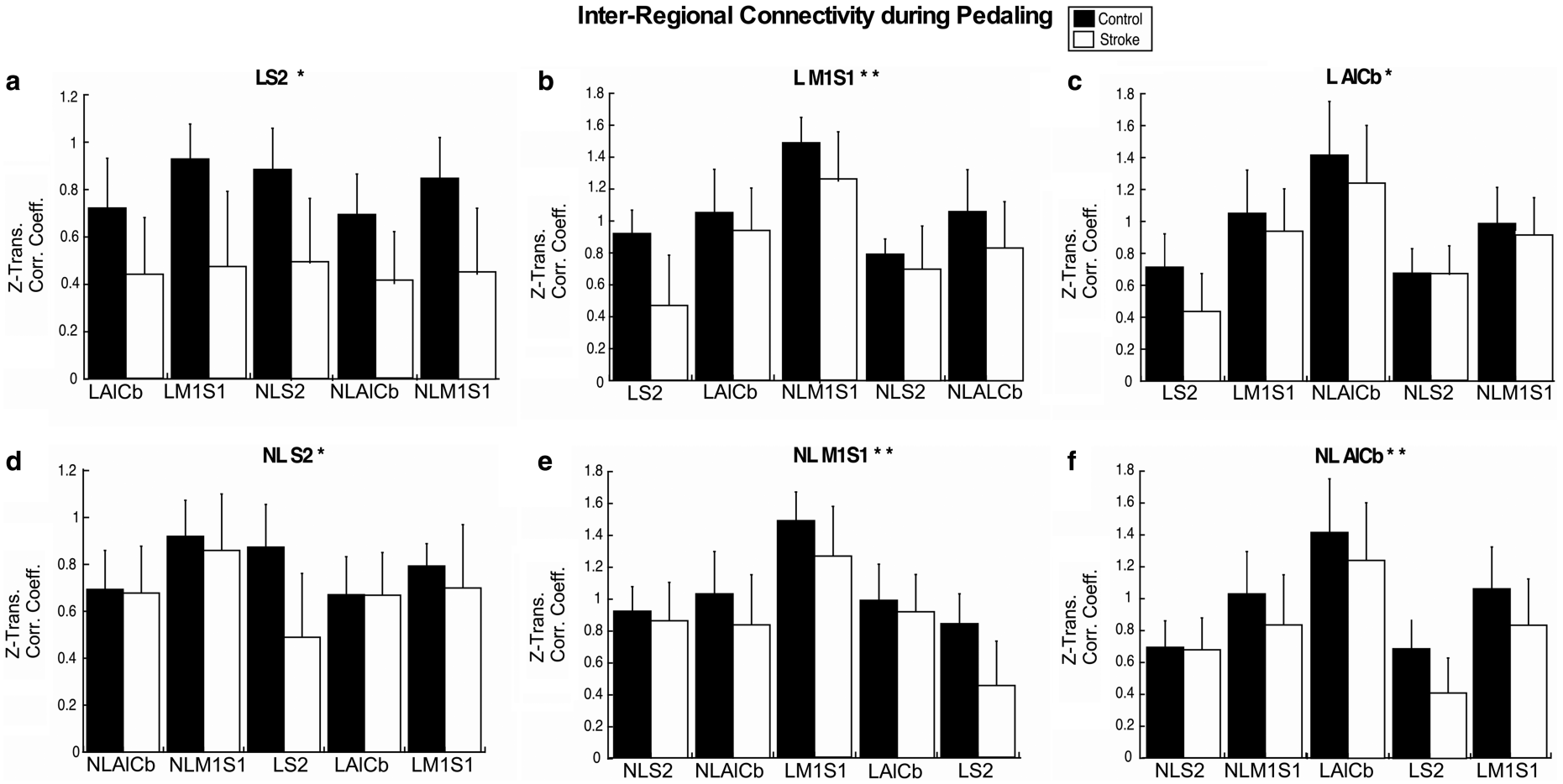

FIG. 3. Inter-regional connectivity during pedaling. Inter-regional connectivity during pedaling for all six task ROI; LS2 **(a)**, L M1S1 **(b)**, L AlCb **(c)**, NLS2 **(d)**, ML M1S1 **(e)**, NL Alcb **(f)**. The task ROI to which sets are anchored is represented in the title of each subplot. Group means (SD) are shown for stroke (white) and control (black) groups. Significant between-group differences are denoted with (*). Significant between-group differences without the L S2 task-ROI are denoted with (**). Values on the *y*-axis are Fischer-Z-transformed correlation coefficients. SD, standard deviation.

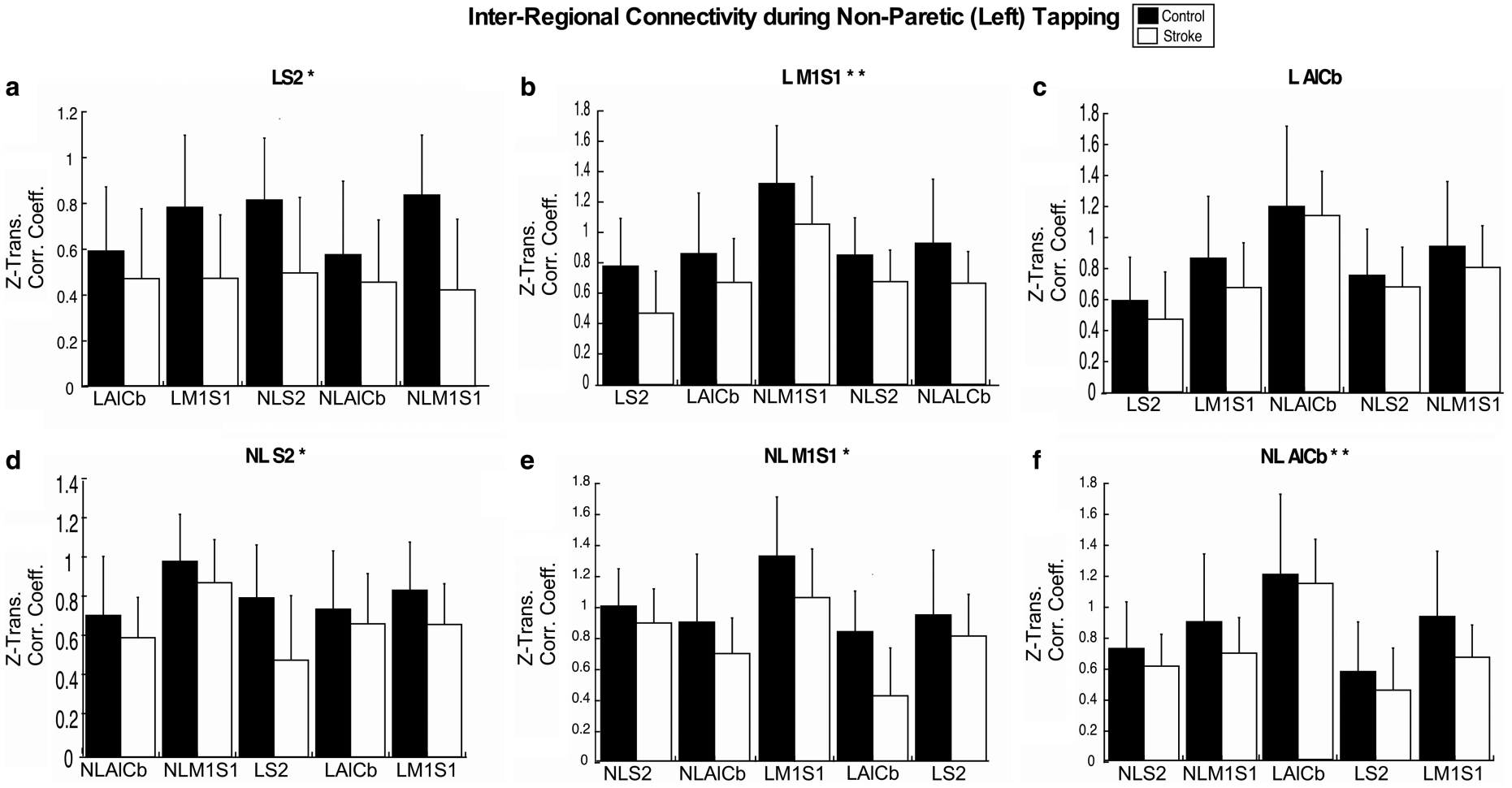

FIG. 4. Inter-regional connectivity during nonparetic tapping. Inter-regional connectivity during nonparetic tapping for all six task ROI; LS2 **(a)**, L M1S1 **(b)**, L AlCb **(c)**, NLS2 **(d)**, ML M1S1 **(e)**, NL Alcb **(f)**. The task ROI to which sets are anchored is represented in the title of each subplot. Group means (SD) are shown for stroke (white) and control (black) groups. Significant between-group differences are denoted with (*). Significant between-group differences without the L S2 task-ROI are denoted with (**). Values on the *y*-axis are Fischer-Z-transformed correlation coefficients.

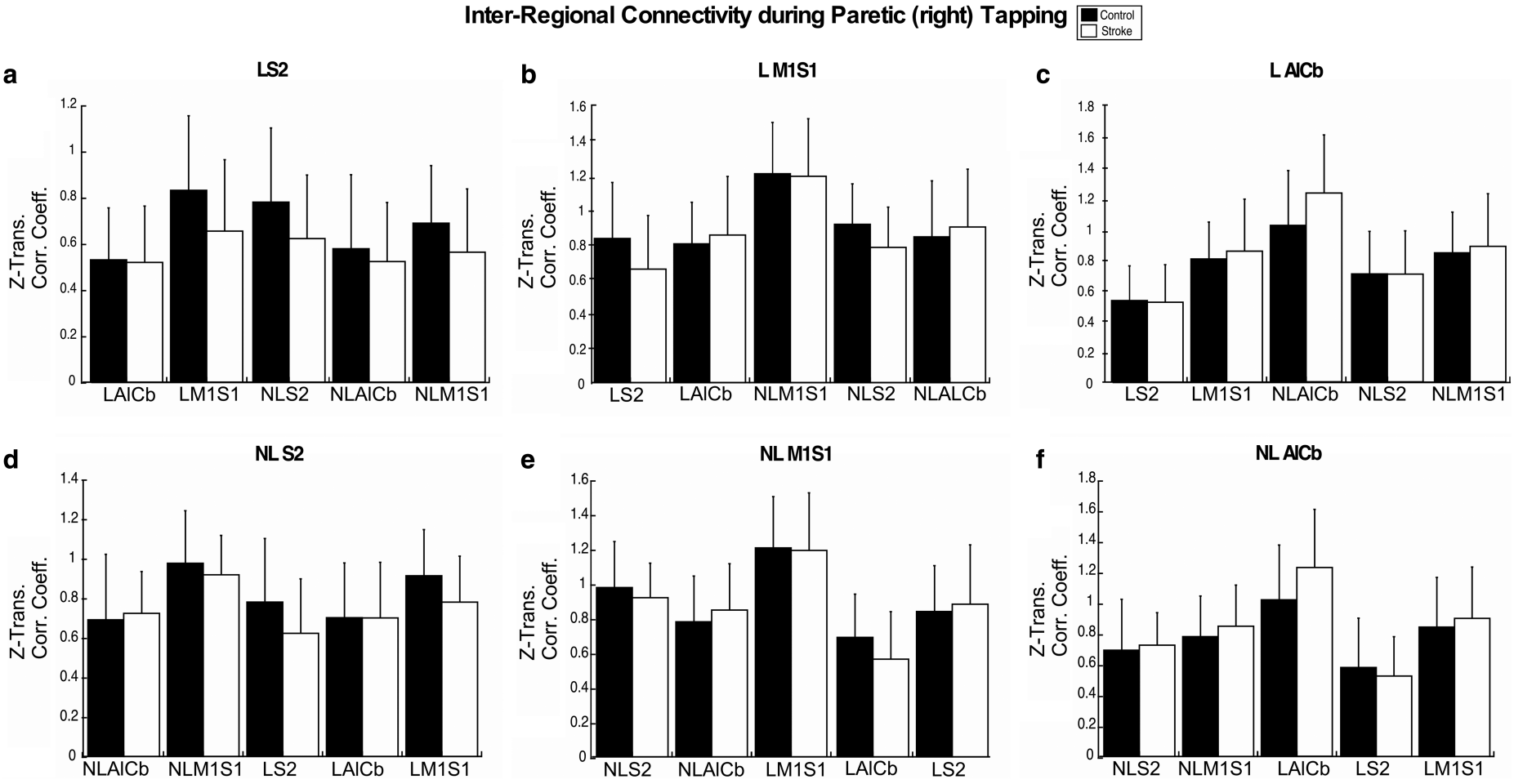

FIG. 5. Inter-regional connectivity during paretic tapping. Inter-regional connectivity during paretic tapping for all six task ROI; LS2 **(a)**, L M1S1 **(b)**, L AlCb **(c)**, NLS2 **(d)**, ML M1S1 **(e)**, NL Alcb **(f)**. The task ROI to which sets are anchored is represented in the title of each subplot. Group means (SD) are shown for stroke (white) and control (black) groups. Values on the *y*-axis are Fischer-Z-transformed correlation coefficients.

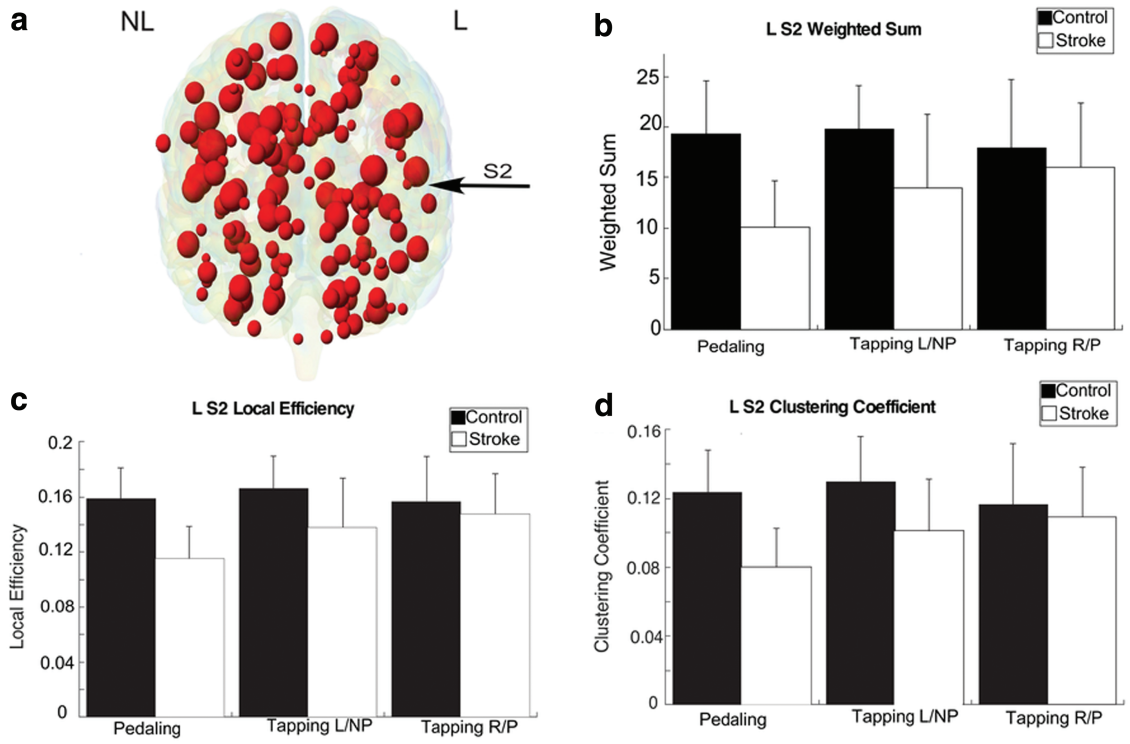

FIG. 6. Topology measurements. Visualization of the 163 nodes used in the topology calculations, with the L S2 task ROI marked by an arrow **(a)**. The L S2 task-ROI was used for the weighted sum **(b)**, local efficiency **(c)**, and clustering coefficient **(d)** calculations. Each bar graph shows the mean (SD) for pedaling (left), nonparetic tapping (middle), and paretic tapping (right) for the control (black) and stroke (white) subjects. Color images are available online.

in controls for all task ROIs ($p \leq 0.015$) except L AlCb ($p = 0.075$). There were no significant interactions ($p \geq 0.736$). The largest effect was in the set anchored to L S2 (ES = 0.160, $p < 0.001$; Fig. 4a). In the other sets with as significant group effect, ES was ≤0.141 ($p < 0.015$; Fig. 4b, e, f). When L S2 was removed due to its large ES, only L M1S2 and NL AlCb were significant (ES ≥0.061, $p < 0.025$; Fig. 4b, f). There were no significant interactions without L S2 ($p \geq 0.414$).

During paretic tapping, there were no significant main effects of group and no group by region interactions associated with inter-regional connectivity ($p \geq 0.057$; Fig. 5).

Between-group differences in topology measures were detected in L S2 only. As shown in Figure 6, there was a significant main effect of group for WS, LE, and CC ($p < 0.001$). No condition ($p \geq 0.153$) or group by condition ($p \geq 0.115$) effects were detected. The largest ESs for all topology measures were seen during pedaling (ES ≥0.47 pedaling, ES <0.20 NP tapping, ES <0.022 for P tapping). When the pedaling condition was removed from analysis, there were no between-group effects for WS ($p = 0.058$), LE ($p = 0.062$), or CC ($p = 0.061$). When the participant with a bilateral lesion (S13) was removed, trends in global connectivity were unchanged. However, inter-regional connectivity for the lesioned cerebellum was no longer significantly different between groups for the pedaling task.

Local connectivity

During pedaling, local connectivity was higher in the control group than the stroke group as evidenced by as significant main effect of group ($p = 0.021$, ES = 0.042) and no significant group by region interaction ($p = 0.097$). During paretic tapping, local connectivity was higher in the stroke than in the control group ($p = 0.002$, ES = 0.074); there was no group by region interaction ($p = 0.938$). Nonparetic tapping showed no between-group effects ($p = 0.520$) or interactions ($p = 0.859$) for local connectivity (Fig. 7). When the participant with bilateral lesion (S13) was removed, still no significant differences were detected in between-group local connectivity.

Clinical correlations

Correlations between stroke-related motor impairment and network function of the brain were examined for FMLE-total, FMLEmotor, FMLEsens, walking velocity, L S2 inter-regional connectivity during pedaling and nonparetic tapping, topology measures during pedaling, and local connectivity during pedaling and paretic tapping. No significant correlations were detected ($p > 0.07$).

Head motion

Mean (SD) values for head motion in the control and stroke groups were 1.58 (0.70) mm and 2.61 (1.40) mm, respectively. An independent *t*-test showed no significant difference between groups ($p = 0.07$).

Discussion

This study provides several novel findings that advance our understanding of network function of the brain after stroke and its relationship to lower limb movement. Consistent

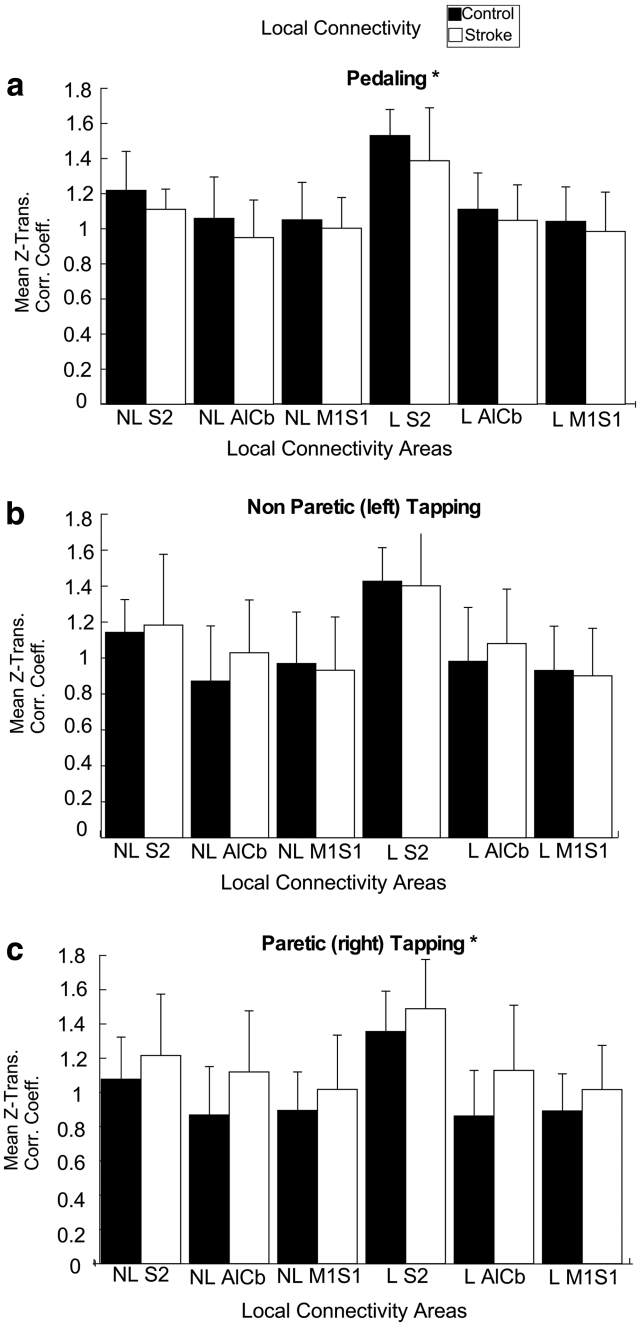

FIG. 7. LC. Bar graphs depicting the local connectivity in all six task ROIs for pedaling **(a)**, nonparetic tapping **(b)**, and paretic tapping **(c)** for control (black) and stroke (white) subjects. Significant between-group differences are denoted with (*).

with our hypothesis, it was found that global network function of the brain was reduced in stroke participants as compared with controls. This reduction was detected during pedaling and nonparetic tapping. It was found that local network function was elevated in stroke participants during paretic tapping and reduced during pedaling. Observations suggest that local and global networks of the brain are altered in chronic stroke; although not always in the same direction. Moreover, the ability to detect changes in functional connectivity after stroke are task-dependent. also discovered the importance of functional connections involving S2, M1S1, and AlCb in lower limb movement after stroke. Results suggest that reduced global connectivity of the brain may contribute to reduced brain activation volume during pedaling poststroke.

Global network connectivity is reduced poststroke; detection is task-dependent

Consistent with our hypothesis, the results of this study demonstrate that global network function of the brain is reduced in people with stroke as compared with controls and that detection of this effect is task-dependent. Inter-regional connectivity among task ROIs was lower in stroke than control participants. This effect was larger during pedaling than nonparetic tapping and was absent during paretic tapping. Topology measures using all regions anchored to L S2 were lower in the stroke than in the control group. This observation was apparent across conditions, but effects were larger during pedaling than tapping.

These results are important because they support and extend an emerging framework suggesting that the effects of stroke are not limited to the site of structural damage. Rather, stroke affects remote, nondamaged brain regions that are part of a functional network. Others have detected this phenomenon as reduced interhemispheric functional connectivity between homo- and heterotopic regions of the cortex (Carter et al., 2010; van Meer et al., 2010), altered effective connectivity within and between hemispheres (Grefkes et al., 2008b), and altered network topology (van Meer et al., 2010). At least one other group has shown that detection of stroke-related changes in global network function is influenced by task (Grefkes et al., 2008a). To date, these conclusions have been drawn from resting-state studies and from task-based paradigms involving upper limb movements and attention. Our work extends this framework to networks influencing lower limb movement.

The nature of pedaling may explain why changes in global connectivity measures in chronic stroke were more sensitive to pedaling than tapping. Tasks that require simultaneous and coordinated movement of both extremities across multiple joints, of which pedaling is one example, probably involve many discrete sensory and motor processing units connected over long distances. Prior work examining the volume and/or intensity of brain activation during pedaling has shown activation in S1, M1, Brodmann's area 6, and cerebellum (Christensen et al., 2000; Fontes et al., 2015; Mehta et al., 2009, 2012; Promjunyakul et al., 2015). Such tasks may require more intensive sensorimotor integration than single-joint movements to ensure that the reciprocal, alternating flexion and extension of each limb occurs at the appropriate point in movement cycle. Thus, pedaling may place higher demands on the sensorimotor network for leg movement, making it more sensitive to stroke-related changes.

Intensive sensorimotor demands associated with pedaling may also explain why the functional connections to S2 were most sensitive to between-group differences in global network function. During pedaling and NP tapping, the largest between-group effect for inter-regional connectivity was for regions anchored to L S2. Between-group differences in topology were limited to connections to L S2. It was

expected to detect effects in other sensory and motor regions (e.g., M1/S1, AlCb), as prior work has shown that these regions are strongly activated by pedaling (Christensen et al., 2000; Mehta et al., 2009, 2012). Moreover, pedaling-related activation volume in these regions is reduced in stroke (Cleland and Schindler-Ivens, 2018; Promjunyakul et al., 2015). However, to date, the importance of S2 in leg movement poststroke has not been identified. S2 is a site of multimodal, interhemispheric sensory integration (Ruben et al., 2001). In humans, there is evidence that it projects to the supplemental and cingulate motor area and to the insula, which has been implicated in motor recovery after stroke (Liao and Yen, 2008; Smith and Alloway, 2013). The reciprocal, bilateral, and multijoint nature of pedaling might place demands on the input/output capacity of S2 that are greater than tapping, which might unmask connectivity deficits involving this region. Regardless of the reason, the marked effect of S2 observed here suggests that the role of this region in leg movement poststroke should continue to be examined.

In this study, nonparetic tapping also revealed inter-regional connectivity deficits for L S2, L M1S1, and NL AlCb. This observation differs from that of Grefkes et al. (2008a), who showed no between-group differences in global connectivity during control and nonparetic hand movements. Conflicting results may be due to differences in the function of the upper and lower limbs. Many important lower limb tasks (e.g., standing, walking) require motor output from both limbs; whereas many upper limb tasks (e.g., using a fork) can be accomplished by one limb. Consequently, global connectivity may be more well developed in sensorimotor networks controlling the legs than the hands. Therefore, even unilateral movements of the lower limbs, such as foot tapping, can activate these networks and reveal stroke-related deficits.

If unilateral lower limb movements activate global networks, then why did nonparetic but not paretic tapping expose between-group differences? Tapping is driven largely by M1. On the NL side of the brain, M1 remains intact and well connected to NL S2 and AlCb. On the lesioned side, connections between M1 and S2 and between M1 and AlCb are likely disrupted. Loss of these connections may render the global network ineffective or make it difficult to activate. Given that tapping is a unilateral movement involving only one joint, the global network may not be essential and, therefore, not activated. Without adequate activation during paretic foot tapping, between-group differences are not detected. It is also curious that nonparetic tapping revealed inter-regional connectivity deficits in L M1/S1, L S2, and NL AlCb. Given that limb movement is contralaterally controlled, one might expect these regions to be minimally active with nonparetic tapping and, therefore, insensitive to between-group differences in global network function. Nonparetic tapping might not activate the global network as effectively as pedaling, whereas activation might be adequate to detect large and consistent between-group differences. These effects would likely involve regions most directly affected by stroke (i.e., LM1/S1, L S2, and NL AlCb).

Local network connectivity is elevated poststroke; detection is task-dependent

Consistent with our hypothesis, the results presented here demonstrate that local network function of the brain may be enhanced by stroke. During paretic tapping, local connectivity within each task ROI was higher in stroke than in control participants. To our knowledge, Yang et al. (2016) is the only other group that has compared local connectivity in people with and without stroke. They also found that the strength of local connections was elevated in stroke as compared with control participants. Observations were made in language networks at rest. Thus, our work supports and extends these conclusions to task-based analysis and sensorimotor networks of the brain. These observations also support the idea that stroke and associated recovery may increase the number or efficacy of short-distance synaptic connections within anatomically distinct regions of the brain via synaptic outgrowth or unmasking of silent synapses. These processes may occur because remaining, intact neurons seek new targets or because they have latent capacity to produce behaviors formerly accomplished by stroke-affected tissue.

Our data also demonstrate that detection of between-group differences in local network strength is task-dependent. Local connectivity within task ROIs was higher in stroke than in control participants during paretic but not nonparetic tapping. During pedaling, local connectivity in the stroke group was lower than in controls. The task-dependency of local connectivity was not predicted from prior work by Smith et al. (2009) that found that resting-state and task-based approaches fully identify local networks of the brain. Though there are no resting-state data, our results are largely in agreement with this work in that all three tasks identified the same six task ROIs, that is, the same network. However, tasks appear to have modulated the strength of the functional connections within each ROI and between ROIs.

The question remains as to why paretic tapping revealed elevated local network function poststroke, whereas pedaling showed an increase and nonparetic tapping showed no difference from controls. Here, it is considered that tapping involves a single joint on one side of the body. Demands for sensorimotor integration within and between hemispheres are minimal. It may be feasible to use a local network to tap the paretic foot, thus exposing stroke-related enhancements in this network. Moreover, the feasibility of performing unilateral movements with a local network may be a driving force for plastic changes that increase the strength of these networks. In contrast to the lesioned cortex, the NL side of the brain and its functional connections remain comparatively intact. Thus, there is no need for enhanced local connectivity during nonparetic tapping, which may explain why this task did not reveal between-group differences. As for pedaling, recall that inter-regional connectivity is reduced in stroke; however, activation of these connections may be imperative for the task. The observation that local connectivity measured during pedaling was lower in stroke than in controls may be due to an interaction between local and global networks. If global connections are excitatory onto local networks, then the loss of global network function poststroke may reduce local connectivity.

Network function of the brain may explain altered activation volume poststroke

This work was motivated by a prior report indicating that brain activation volume during pedaling was lower in people with stroke than in controls. During paretic foot tapping,

people with stroke have higher brain activation volume than controls. This study examined whether task-related differences in activation volume were related to network function of the brain. It was hypothesized that reduced activation volume during pedaling may be due to loss of global network function of the brain, whereas increased brain activation during tapping may be due to elevated local network function. The present data provide support for this hypothesis. Global network function, as measured by inter-regional connectivity and topology, was lower in the stroke than in the control group. This observation was most robust during pedaling. Hence, the loss of global network function and subsequent reductions in excitatory drive to local networks may explain why brain activation volume was reduced during pedaling. Measures of local network function of the stroke-affected brain were as large or larger than controls during the tapping tasks. Normal or enhanced local network function may explain why activation volume of the stroke-affected brain was not reduced—and was even somewhat elevated—during paretic tapping. These observations also suggest that tasks involving coordinated movement of both legs and/or multiple joints may be needed to detect changes in global network function of the brain. In contrast, unilateral, single-joint tasks may expose changes in local networks. The task-dependent nature of our findings may also explain why most prior studies report elevated brain activation in people with stroke, whereas our pedaling work revealed decreased activation volume. Most prior work has examined brain activation intensity and volume during flexion and extension movements of a single joint on one side of the body. These movement paradigms may activate local networks more effectively than global networks, which preferentially exposes changes in local sensorimotor networks involved in movement.

Limitations

Although the registration method used here (i.e., ANTs) has been validated for stroke participants (Avants et al., 2011), it does not align anatomic regions in subject space to the reference brain with complete accuracy. Regions around the lesion are particularly susceptible to registration error. Thus, the ROIs that were identified provide an imperfect representation of the underlying anatomy, and group data may be blurred by between-subject variation. Head motion is another concern, as increased head motion during pedaling could account for reduced global connectivity in the stroke group. This confound is unlikely because head motion was within acceptable limits (Seto et al., 2001) and was not different between groups. It is also possible that task-related effects on local and global connectivity were due to the experimental design. Tapping was done with an event-related design, whereas pedaling was done in blocks. Moreover, task-related changes in the fMRI time series may not have been fully removed, and results may be influenced by task-related changes in the fMRI time series. Conclusions are also limited in terms of generalizability and risk of type II error, as our sample was a heterogenous group of only 15 stroke and 8 control participants. Future work will target larger samples to confirm or refute our conclusions and determine whether they hold across stroke severity and type. Finally, our task-related conclusions should be viewed with caution, as resting-state connectivity analyses were not done. The extent to which it was concluded that our results are task-dependent should be constrained to task-based functional connectivity, not resting state. Future work should examine these constructs during tasks and resting state.

Conclusion

This study showed that global network function of the brain was lower in people with stroke as compared with controls. Effects were larger during pedaling than foot tapping. It was also found that local network function was higher in stroke participants than controls, but this effect was detected only during paretic foot tapping. These observations illustrate that detection of altered network function of the brain is task-dependent. Moreover, differential changes in local and global networks poststroke may explain why brain activation volume is reduced during pedaling, but not tapping.

Acknowledgments

Dr. Naveen Bansal provided guidance with the statistics. Dr. Nutta-on Promjunyakul collected the data. This work was funded by grants from the National Center for Medical Rehabilitation Research within the Eunice Kennedy Shriver National Institute of Child Health and Human Development (Grant No. HD060693; S.S.I.) and Advancing a Healthier Wisconsin, Research and Education Program.

Author Disclosure Statement

No competing financial interests exist.

Supplementary Material

Supplementary Figure S1

References

Avants BB, Tustison NJ, Song G, Cook PA, Klein A, Gee JC. 2011. A reproducible evaluation of ANTs similarity metric performance in brain image registration. Neuroimage 54: 2033–2044.

Biswal B, Yetkin FZ, Haughton VM, Hyde JS. 1995. Functional connectivity in the motor cortex of resting human brain using echo-planar MRI. Magn Reson Med 34:537–541.

Calautti C, Baron J. 2003. Functional neuroimaging studies of motor recovery after stroke in adults: a review. Stroke 34: 1553–1566.

Carey J, Anderson K, Kimberley T, Lewis S, Auerbach E, Ugurbil K. 2004. fMRI analysis of ankle movement tracking training in subject with stroke. Exp Brain Res 154:281–290.

Carter AR, Astafiev SV, Lang CE, Connor LT, Rengachary J, Strube MJ, et al. 2010. Resting interhemispheric functional magnetic resonance imaging connectivity predicts performance after stroke. Ann Neurol 67:365.

Christensen LO, Johannsen P, Sinkjaer T, Petersen N, Pyndt HS, Nielsen JB. 2000. Cerebral activation during bicycle movements in man. Exp Brain Res 135:66–72.

Cleland BT, Schindler-Ivens S. 2018. Brain activation during passive and volitional pedaling after stroke. Motor Control 23:1–29.

Cox RW. 1996. AFNI: software for analysis and visualization of functional magnetic resonance neuroimages. Comput Biomed Res 29:162–173.

Cramer SC, Nelles G, Benson RR, Kaplan JD, Parker RA, Kwong KK, et al. 1997. A functional MRI study of

subjects recovered from hemiparetic stroke. Stroke 28:2518–2527.

Enzinger C, Johansen-Berg H, Dawes H, Bogdanovic M, Collett J, Guy C, et al. 2008 Functional MRI correlates of lower limb function in stroke victims with gait impairment. Stroke 39: 1507–1513.

Fontes EB, Okano AH, De Guio F, Schabort EJ, Min LL, Basset FA, et al. 2015. Brain activity and perceived exertion during cycling exercise: an fMRI study. Br J Sports Med 49:556–560.

Fridman EA, Hanakawa T, Chung M, Hummel F, Leiguarda RC, Cohen LG. 2004. Reorganization of the human ipsilesional premotor cortex after stroke. Brain 127:747–758.

Fugl-Meyer AR, Jääskö L, Leyman I, Olsson S, Steglind S. 1975. The post-stroke hemiplegic patient. 1. A method for evaluation of physical performance. Scand J Rehabil Med 7:13–31.

Grefkes C, Eickhoff SB, Nowak DA, Dafotakis M, Fink GR. 2008a. Dynamic intra- and interhemispheric interactions during unilateral and bilateral hand movements assessed with fMRI and DCM. Neuroimage 41:1382–1394.

Grefkes C, Nowak DA, Eickhoff SB, Dafotakis M, Küst J, Karbe H, Fink GR. 2008b. Cortical connectivity after subcortical stroke assessed with functional magnetic resonance imaging. Ann Neurol 63:236–246.

Johansen-Berg H, Rushworth MFS, Bogdanovic MD, Kischka U, Wimalaratna S, Matthews PM. 2002. The role of ipsilateral premotor cortex in hand movement after stroke. Proc Natl Acad Sci U S A 99:14518–14523.

Kim YH, You SH, Kwon YH, Hallett M, Kim JH, Jang SH. 2006. Longitudinal fMRI study for locomotor recovery in patients with stroke. Neurology 67:330–333.

Liao C, Yen C. 2008. Functional connectivity of the secondary somatosensory cortex of the rat. Anat Rec 291:960–973.

Mehta JP, Verber MD, Wieser JA, Schmit BD, Schindler-Ivens SM. 2009. A novel technique for examining human brain activity associated with pedaling using fMRI. J Neurosci Methods 179:230–239.

Mehta JP, Verber MD, Wieser JA, Schmit BD, Schindler-Ivens SM. 2012. The effect of movement rate and complexity on functional magnetic resonance signal change during pedaling. Motor Control 16:158–175.

Minka TP. 2001. Automatic choice of dimensionality for PCA. In: Leen TK, Dietterich TG, Tresp V (eds.) *NIPS 13*. Cambridge, MA: MIT Press; pp. 598–604.

Promjunyakul N, Schmit BD, Schindler-Ivens SM. 2015. A novel fMRI paradigm suggests that pedaling-related brain activation is altered after stroke. Front Hum Neurosci 9:324.

Pruim RHR, Mennes M, van Rooij D, Llera A, Buitelaar JK, Beckmann CF. 2015. ICA-AROMA: a robust ICA-based strategy for removing motion artifacts from fMRI data. Neuroimage 112:267–277.

Roy AK, Shehzad Z, Margulies DS, Kelly AMC, Uddin LQ, Gotimer K, et al. 2009. Functional connectivity of the human amygdala using resting state fMRI. Neuroimage 45: 614–626.

Ruben J, Schwiemann J, Deuchert M, Meyer R, Krause T, Curio G, et al. 2001. Somatotopic organization of human secondary somatosensory cortex. Cereb Cortex 11:463–473.

Rubinov M, Sporns O. 2010. Complex network measures of brain connectivity: uses and interpretations. Neuroimage 52:1059–1069.

Seto E, Sela G, McIlroy WE, Black SE, Staines WR, Bronskill MJ, et al. 2001. Quantifying head motion associated with motor tasks used in fMRI. Neuroimage 14:284–297.

Smith JB, Alloway KD. 2013. Rat whisker motor cortex is subdivided into sensory-input and motor-output areas. Front Neural Circuits 7:4.

Smith S, Fox P, Miller K, Glahn D, Fox M, Mackay C, et al. 2009. Correspondence of the brain's functional architecture during activation and rest. Proc Natl Acad Sci U S A 106: 13040–13045.

Smith SM, Jenkinson M, Woolrich MW, Beckmann CF, Behrens TEJ, Johansen-Berg H, et al. 2004. Advances in functional and structural MR image analysis and implementation as FSL. Neuroimage 23:S219.

Urbin MA, Hong X, Lang CE, Carter AR. 2014. Resting-state functional connectivity and its association with multiple domains of upper-extremity function in chronic stroke. Neurorehabil Neural Repair 28:761–769.

van Meer MPA, van der Marel K, Wang K, Otte WM, El Bouazati S, Roeling TAP, et al. 2010. Recovery of sensorimotor function after experimental stroke correlates with restoration of resting-state interhemispheric functional connectivity. J Neurosci 30:3964–3972.

Westlake KP, Nagarajan SS. 2011. Functional connectivity in relation to motor performance and recovery after stroke. Front Systems Neurosci 5:8.

Yang M, Li J, Li Y, Li R, Pang Y, Yao D, et al. 2016. Altered intrinsic regional activity and interregional functional connectivity in post-stroke aphasia. Sci Rep 6:24803.

Yu-Feng W, Yu-Feng Z, Yong H, Chao-Zhe Z, Qing-Jiu C, Man-Qiu S, et al. 2007. Altered baseline brain activity in children with ADHD revealed by resting-state functional MRI. Brain Dev 29:83–91.

Address correspondence to:
Kaleb Vinehout
Department of Biomedical Engineering
Marquette University and the Medical College of Wisconsin
Olin Engineering Center, Room 206
Milwaukee, WI 53201-1881

E-mail: kvinehout@mcw.edu